Chemical Engineering Science 64 (2009) 1027 – 1035

Contents lists available at ScienceDirect

Chemical Engineering Science

journal homepage: www.elsevier.com/locate/ces

Percutaneous absorption of volatile solvents following transient liquid exposures: I. Model development

Siladitya Ray Chaudhuri[a], Gerald B. Kasting[b,*], William B. Krantz[c]

[a]Department of Chemical and Materials Engineering, University of Cincinnati, Cincinnati, OH 45221-0012, USA
[b]James L. Winkle College of Pharmacy, University of Cincinnati Academic Health Center, 3225 Eden Avenue, Cincinnati, OH 45267-0004, USA
[c]Department of Chemical and Biomolecular Engineering, National University of Singapore, 117576, Republic of Singapore

ARTICLE INFO

Article history:
Received 16 May 2008
Received in revised form 8 August 2008
Accepted 21 August 2008
Available online 5 September 2008

Keywords:
Mass transfer
Mathematical modeling
Percutaneous absorption
Transient exposure
Scaling analysis
Skin
Volatile liquids
Transdermal transport

ABSTRACT

A one-dimensional mass-transport model describing the disposition of a volatile liquid applied topically to human skin in vitro is described. The physical model consists of three layers—the vehicle (VH), stratum corneum (SC) and viable tissues (VT). Each layer is considered to be homogeneous except for the uppermost portion of the SC, which is considered to be peeling off in scales or desquamating and is subject to almost instantaneous capillary sorption during the initial application of liquid. This behavior is captured by a parameter defined as the fractional deposition depth f_{dep}. Its influence is shown here by means of parametric simulation studies. The diffusion/evaporation model is described and analyzed from a scaling approach, and solved for the case of a permeant having the properties of ethanol, a common solvent for the deposition of solutes on skin, using a finite difference/finite element code that allows for the moving boundary problem associated with the VH. The advantages relative to prior computational models for percutaneous absorption are that this improved model can readily be extended to describe the skin disposition of solutes from binary or multi-component mixtures or to describe combined heat and mass transfer in skin, two problems that have not been quantitatively addressed heretofore.

1. Introduction

Although all life forms depend upon membrane-like structures for their existence, nowhere is this more dramatically demonstrated than in the skin (Potts and Francoeur, 1991). Skin is the largest organ in the human body, covering a surface area of approximately $2\,m^2$ and receiving about one-third of the total circulating blood (Singh and Singh, 1993). Owing to its immediate proximity to the environment, skin is naturally exposed to a variety of chemical compounds. As a semi-permeable membrane, it can serve as a possible entry point for a host of therapeutic substances, which serves as the core concept in transdermal drug delivery. However, many of these substances have the potential of interacting adversely with the skin or with the internal physiological systems. Hence, the disposition of chemical compounds in contact with human skin has evoked substantial research interest.

The different ways of modeling transport through human skin can be broadly classified as being either mechanistic or non-mechanistic, and either transient or steady-state. A general review of the steady-state methods along with a critical comparison has been made by Yamashita and Hashida (2003). The most influential among these steady-state methods was introduced by Potts and Guy (1992), who considered skin as a structured lipid membrane characterized by an octanol-like chemical environment and a strong dependence of diffusivity on the molecular weight of the permeant. Potts and Guy provided the first quantitative analysis of a large human skin permeability database collected by Flynn (1990). Many variations on this approach have been proposed, often involving sets of chemical descriptors that are more complex than just molecular weight or diffusivity. Collectively, they are called quantitative structure permeability relationships (QSPRs). Comprehensive critical analyses of QSPRs have been provided by Geinoz et al. (2004) and Moss et al. (2002). Transient skin permeation models were pioneered by Scheuplein (1965) and Scheuplein and Blank (1971) and comprise both diffusion models and compartmental pharmacokinetic approaches. An excellent summary of pioneering work in this field can be found in the works of McCarley and Bunge (2001). Since then, considerable progress has been made by several research groups (Anissimov and Roberts, 2001, 2004; Barbero and Frasch, 2005; Frasch, 2002; Frasch and Barbero, 2003; Kasting, 2001; Kasting and Miller, 2006). It should be noted that most of these approaches have involved non-volatile compounds applied in limited doses to

* Corresponding author. Tel.: +1 513 558 1817; fax: +1 513 558 0978.
E-mail addresses: Gerald.Kasting@uc.edu, gkasting@cinci.rr.com (G.B. Kasting).

0009-2509/$ - see front matter © 2008 Published by Elsevier Ltd.
doi:10.1016/j.ces.2008.08.021

human skin. All of these models consider passive diffusion as the primary transport process in skin and the stratum corneum (SC) as the rate-limiting barrier for most permeants. These assumptions are consistent with a large body of experimental data and may be considered as well established (Scheuplein and Blank, 1971).

Studies on skin absorption of volatile compounds are less common. These include vapor phase (Del-Valle et al., 2004; Jakasa et al., 2004; Kezic et al., 2000) and liquid-phase absorption (Batterman and Franzblau, 1997; Larese Filon et al., 1999; Korinth et al., 2003; Lockley et al., 2004; Mráz and Nohová, 1992; Semple et al., 2001; Stinchcomb et al., 1999; Wilkinson and Williams, 2002). However, these researchers do not perform a quantitative analysis of their data using diffusion models. In order to bridge the gap between diffusion modeling and experimental skin permeation data on pure volatile liquids, Kasting and Miller (2006) proposed a diffusion model (henceforth referred to as the KM model) that represented the disposition of an arbitrary dose of a (potentially) volatile compound applied to skin. Although the KM model was sophisticated in some respects, it contained simplifications in order to focus attention on the key aspects of volatility and skin solubility of the permeant. In some cases, these simplifications led to the development of closed-form analytical solutions. This article attempts to assess the validity of these approximations and remove some of them in order to develop a more comprehensive model.

One significant simplification in the KM model was the omission of viable tissue (VT) (epidermis and dermis) as a participating skin layer. This effectively limited the analysis of compounds for which the (base 10) logarithm of the octanol–water partition coefficient ($K_{oct/w}$) was less than 3.0 (Cleek and Bunge, 1993). This restriction can be removed by the methods discussed by Anissimov and Roberts (2001) or by adding an explicit VT layer, but at a loss of the relatively simple closed-form solutions (Kasting and Miller, 2006). Thus, the model to be described in this paper includes VT as a participating layer, thereby making it a multi-layer model. This means that instead of a single partial differential equation (PDE), the model consists of a system of PDEs with coupled boundary conditions (BCs) at the common interfaces. Another assumption of the KM model involved the concept of a 'deposition layer' in the upper SC, a layer into which some of the compound of interest was immediately sorbed by capillary action. This assumption followed from structural observations that the upper 1–3 μm of SC is in the process of desquamation and has lost much of its lipid content. This concept of a deposition region can be replaced by an instantaneous equilibrium at the liquid–skin interface combined with a high diffusivity in the upper SC. This concept of a deposition depth is revisited in detail in this paper.

Another feature not included in the KM model is convection or bulk flow of permeants in each layer. Convection is an integral component of mass transfer and is present even in the absence of explicit fluid flow in the system (owing to a pressure drop and/or other external driving forces) (Bear and Bachmat, 1990). This concept of convection arising purely from concentration gradients or density gradients for binary or higher systems is called diffusion-induced convection or convection due to densification. Convection is inherently associated with diffusive transport, although it is not always significant (Cussler, 1997). It becomes progressively more important as the solute concentration increases. Convection has previously been considered in modeling transport through polymeric membranes (Alsoy and Duda, 2002) and in polymeric membrane formation via evaporative casting (Lee et al., 2006). If the saturation solubility or maximum concentration for a permeant in a skin layer is small, then diffusion-induced convection can be neglected. This assumption is commonly referred to as the 'dilute solution approximation'. However, if the skin concentrations are large, then omission of convection can lead to erroneous results. In other words, convection should be included in a generalized predictive mass-transport model representing skin disposition of chemical compounds and has been incorporated into the model developed in this paper.

A final feature not included in the KM model was heat transfer effects. We studied this problem experimentally by measuring the surface temperature of ethanol-treated skin with an infrared thermometer (data not shown) and determined that the maximum change in the forearm skin temperature using a laboratory fan to accelerate evaporation was about 2 °C. The change was not large enough to warrant development of a combined heat- and mass-transfer model; consequently the present model is isothermal.

2. Development of the model equations

The concurrent evaporation–absorption process is shown schematically in Fig. 1. It involves the application of a known amount of pure volatile liquid on the top of the skin forming an explicit vehicle layer (VH) of initial thickness L_0. Structurally, human skin is a highly stratified barrier with complex structural and physiological aspects (Bouwstra et al., 2002; Menon, 2002; Montagna et al., 1992; Roberts and Walters, 1998). It consists of two main layers: epidermis and dermis. The lower layer, dermis, forms the bulk of skin and is highly vascular, containing active capillaries. The top layer, epidermis, is devoid of blood vessels and can in turn be subdivided into several distinct sublayers. The structure and function of the individual epidermal layers have been extensively discussed by Menon (2002). Most importantly, it has been established that the outermost epidermal layer, the non-viable SC is the principal barrier to transdermal transport for most compounds (Blank, 1964; Scheuplein, 1965; Scheuplein and Blank, 1971). Accordingly, the current model considers skin to be a two-layered membrane. The top layer is the more resistive SC (having thickness L_{SC}) while the bottom layer, henceforth referred to as VT and having thickness L_{VT}, represents viable epidermis and a fraction of the dermis unperfused, that is, devoid of blood vessels. The proposed model does not consider either swelling or shrinking resulting from intermolecular interaction between the permeant and the skin; hence the skin layer thicknesses remain constant throughout the permeation process. However, for material balance purposes, the amount of permeating liquid is included in recalculating the initial SC thickness. The origin of the spatial coordinate system lies at the SC–VT interface. When a VH layer is present, the volatile compound dissipates from this layer via two simultaneous mechanisms. At the liquid–gas interface, the compound is lost by evaporation, while at the VH–SC interface it

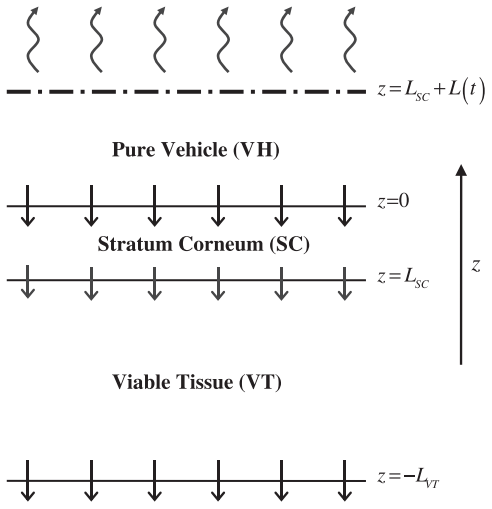

Fig. 1. Schematic of the evaporation–absorption process for a volatile liquid permeant deposited on skin.

penetrates via diffusion (and convection) into the SC. This results in the thinning of the VH film whose thickness is denoted by $L = L(t)$. When the VH completely disappears, the system is reduced to a simpler two-layer model. The compound now desorbs from the SC and VT layers, respectively, through evaporation at the newly formed SC–air interface and clearance at the lower boundary of the VT.

We adopt the concept of a deposition layer as described in Kasting and Miller (2006). This solvent deposition is assumed to be instantaneous, which is a reasonable assumption for volatile solvents since the time scale for capillary sorption is much shorter than that for diffusive transport. The amount of compound deposited into a unit area of SC is given by the product of the saturation concentration of the compound in the SC and the depth of the solvent-deposited region (henceforth referred to as the deposition depth). The net amount of liquid left in the VH is the difference between the initial amount applied and the amount deposited into the SC. The entire system is assumed to be isothermal at 32 °C.

The general conservation equation for mass transport through an arbitrary barrier layer LY can be written as

$$\frac{\partial \rho_P^{\mathrm{LY}}}{\partial t} = -\frac{\partial n_P^{\mathrm{LY}}}{\partial z} \tag{1}$$

where t is the time, z is the spatial coordinate, ρ_P^{LY} and n_P^{LY}, respectively, denote the mass concentration and total mass flux with respect to a stationary reference frame of the permeant in a particular layer (LY = SC, VT). By definition, the mass concentration is a product of the mass fraction (ω_P^{LY}) and the total solution (layer) density. It can be written as

$$\rho_P^{\mathrm{LY}} = \omega_P^{\mathrm{LY}} \rho^{\mathrm{LY}} \tag{2}$$

Since the SC and VT are assumed to be immobile phases, the mass flux with respect to a stationary reference frame of a permeant through these layers can be written as (Bird et al., 1960):

$$n_P^{LY} = \frac{j_P^{\mathrm{LY}}}{1 - \omega_P^{\mathrm{LY}}} \tag{3}$$

where j_P^{LY} is the diffusive mass flux of the permeant with respect to the mass–average velocity. The diffusive mass flux can be expressed in terms of Fick's first law of diffusion (Bird et al., 1960) as

$$j_P^{\mathrm{LY}} = -\rho^{\mathrm{LY}} D_{\mathrm{PLY}} \frac{\partial \omega_P^{\mathrm{LY}}}{\partial z} \tag{4}$$

where D_{PLY} is the diffusivity of the permeant inside the LY. Thus, the governing equations describing mass transport of the permeant in the SC and VT, respectively, are given by

$$\frac{\partial \omega_P^{SC}}{\partial t} = D_{\mathrm{PSC}} \frac{\partial}{\partial z}\left[\frac{1}{(1-\omega_P^{SC})} \frac{\partial \omega_P^{SC}}{\partial z}\right] \tag{5}$$

$$\frac{\partial \omega_P^{VT}}{\partial t} = D_{\mathrm{PVT}} \frac{\partial}{\partial z}\left[\frac{1}{(1-\omega_P^{VT})} \frac{\partial \omega_P^{VT}}{\partial z}\right] \tag{6}$$

In deriving Eqs. (5) and (6), the diffusion coefficients in both the SC and VT have been assumed to be constant since information on the concentration dependence of the diffusion coefficients is unavailable; however, relaxing this assumption in the model can be accommodated if this information is supplied. Furthermore, the dimensions and densities of the SC and VT have been assumed to be constant over time. The amount of liquid absorbed almost instantaneously into the top layer of the SC was used to recalculate the initial thickness of the SC. This is a simplified description of the system that ignores the transient swelling phenomenon in the SC associated with the absorption of a topically applied solute. Accurate models for this phenomenon are not available and remain the subject of ongoing research. Eqs. (5) and (6) are non-linear second-order PDEs, each requiring one initial condition (IC) and two BCs for a particular solution. The IC for the PDEs is given by a known initial concentration of permeant in these layers. For the VT, this is equal to zero:

$$\omega_P^{VT}|_{z,0} = 0 \tag{7}$$

The presence of the solvent-deposited region in the SC means that a fraction of the SC will have a non-zero concentration in the beginning. This approximation is based on a presumed separation of time scales between filling of the deposition region by capillary sorption (seconds) and diffusive permeation through the SC (tens of minutes) (Kasting and Miller, 2006). The IC can be written as

$$\omega_P^{SC}|_{z,0} = 0 \quad \text{for } 0 \leqslant z < (1 - f_{\mathrm{dep}}) L_{SC} \tag{8}$$

$$\omega_P^{SC}\big|_{z,0} = \omega_{\mathrm{sat}}^0 \quad \text{for } (1 - f_{\mathrm{dep}}) L_{SC} \leqslant z \leqslant L_{SC} \tag{9}$$

where f_{dep} is the fractional deposition depth and ω_{sat}^0 is the saturation composition. The bottom of the VT has a sink condition at which the permeant concentration goes to zero. This is representative of in vivo situations for which the permeant is completely cleared by a network of blood capillaries or the in vitro situation, for which it is flushed away by circulating buffer solution. This condition can be written as

$$\omega_P^{VT}|_{-L_{VE},t} = 0 \tag{10}$$

The BC at the top of the SC will depend on the presence or absence of the VH (as discussed above) and is given by

$$\omega_P^{SC}|_{L_{SC},t} = K_{SC/VH}^P \frac{\rho_P^o}{\rho^{SC}} \quad \text{for } 0 \leqslant t \leqslant t_{\mathrm{depl}} \tag{11}$$

$$n_P^{SC}|_{L_{SC},t} = n_P^G|_{L_{SC},t} \quad \text{for } t > t_{\mathrm{depl}} \tag{12}$$

where $K_{SC/VH}^P$ and ρ_P^o denote the SC/VH partition coefficient and the pure component mass density of the permeant, respectively; n_P^G is the mass flux of the permeant into the surrounding air phase; and t_{depl} is the time required for the VH to completely disappear. These relationships are used in conjunction with appropriate evaporation mass-transfer relationships (Eqs. (17) and (18)) to ensure continuity of mass concentration and flux as the VH dissipates. The BCs at the SC–VT interface remain the same at all times and are given by a partition relation and continuity of flux:

$$\omega_P^{SC}|_{0,t} = \frac{\rho^{VT}}{K_{VT/SC}^P \rho^{SC}} \omega_P^{VT}|_{0,t} \tag{13}$$

$$n_P^{VT}|_{0,t} = n_P^{SC}|_{0,t} \tag{14}$$

Finally, since the VH layer consists of a single component, an instantaneous material balance on this layer results in an ODE (instead of a PDE) and is written as

$$\rho_P^o \frac{\mathrm{d}L}{\mathrm{d}t} = -n_P^G + n_P^{SC}|_{z=L_{SC}} \tag{15}$$

where $\mathrm{d}L/\mathrm{d}t$ is the velocity of the liquid–gas interface. Eq. (15) is coupled with Eqs. (5) and (6) and needs an IC. This is given by the initial thickness of the VH:

$$L(0) = L_0 \tag{16}$$

In order to complete the description of the model, an expression for the gas-phase flux of the permeant from the VH is required. The

simplest description involves the use of a lumped parameter or mass-transfer coefficient. The expressions for the gas-phase flux from the VH and SC are given by Eqs. (17) and (18), respectively:

$$n_P^G = k_{\text{evap}}\rho_P^0 \tag{17}$$

$$n_P^G|_{L_{SC},t} = k_{\text{evap}}\rho_P^0\frac{\omega_P^{SC}|_{L_{SC},t}}{\omega_{\text{sat}}^0} \tag{18}$$

where k_{evap} is the evaporative mass-transfer coefficient describing permeant flux into the ambient gas phase. Eq. (18) assumes that the maximum evaporation rate from the surface of a permeant soaked SC cannot be greater than the evaporation rate from the free surface of the liquid itself. When $\omega_P^{sc}|_{L_{SC}} = \omega_{\text{sat}}^0$, the evaporation rate in Eq. (18) is exactly the same as Eq. (17), thereby maintaining a continuity of evaporation rates as observed through experiments. Thus, Eq. (15) can be rewritten as

$$\rho_P^0\frac{\mathrm{d}L}{\mathrm{d}t} = -k_{\text{evap}}\rho_P^0 + \left.\frac{-\rho^{sc}D_{\text{PSC}}}{1-\omega_P^{SC}}\frac{\partial\omega_P^{sc}}{\partial z}\right|_{z=L_{SC}} \tag{19}$$

The one-dimensional nature of the model described here warrants a comment. The surface roughness of healthy skin is comparable to the thickness of the SC and varies with site and age (Fujimura et al., 2007), resulting in a microscopic surface area that is quite variable and substantially larger than the apparent surface area (Fischer et al., 1999; Fiedler et al., 1995). Furthermore, there is three-dimensional structural variation within the VT layer, as it is comprised of viable epidermis and dermis, which have a complex interface involving a pattern of ridges (the so-called Reti ridges) (Montagna et al., 1992). Our working approximation is that viable epidermis and dermis have similar transport properties (Kasting et al., 2008), eliminating the need to describe the latter variation. The surface roughness effect is accommodated in the present model by calibration of the evaporative mass-transfer coefficient, k_{evap}, versus experimental data. The microscopic dynamics are effectively averaged by this process.

3. Approximation (scaling) analysis of model equations

The differential equations for any (transport) model can be analyzed to assess the importance of each phenomenon involved in the process. This is known as an 'approximation analysis' and its merit has been identified by several researchers (Bear and Bachmat, 1990; Deen, 1998; Krantz, 1970, 2007). Here, this is done using scaling analysis, which involves non-dimensionalizing the describing equations so that the significant terms are scaled to be of order one, which leads to a minimum parametric representation of the process. The resulting dimensionless groups that appear in the dimensionless describing equations permit assessing the importance of the terms (such as the unsteady-state or convective transport terms) with which they are associated. This systematic technique of scaling analysis has been discussed in detail by Krantz (1970, 2007) and Krantz and Sczechowski (1994). The advantage of scaling analysis is that it provides general criteria in terms of dimensionless groups that must be very small in order to justify certain assumptions in the describing equations.

For the given problem, the independent and dependent variables are non-dimensionalized in terms of the following parameters (known as scale factors):

$$t^* = \frac{t}{t_o},\quad z_{SC}^* = \frac{z}{L_{SC}},\quad z_{VT}^* = \frac{z}{L_{VT}}\quad\text{and}\quad L^* = \frac{L}{L_0} \tag{20}$$

In Eq. (20), t_o is the observation time, which is taken to be the duration of the dynamic process such that t^* is always scaled between 0 and 1. L_{SC}, L_{VT} and L_0 serve as the scale factors for the SC, VT and (initial) vehicle thicknesses. Although the mass fraction is a dimensionless quantity, a separate scale factor (for each layer) is introduced in order to restrict its value to be between 0 and 1. This substitution puts a bound on the magnitude of the mass fraction for even a dilute component to $o(1)$. When a separate scale factor is introduced for the mass fraction of one component, the scale factor for the mass fraction for the other component (its complement) is taken to be unity.

$$\omega_{\text{PSC}}^* = \frac{\omega_P^{SC}}{(K_{SC/VH}^P\rho_P^0/\rho^{SC})}\quad\text{and}\quad \omega_{\text{PVT}}^* = \frac{\omega_P^{VT}}{(K_{VT/SC}^P K_{SC/VH}^P\rho_P^0/\rho^{VT})} \tag{21}$$

The interfacial displacement velocity is scaled with an independent scale factor (and not as thickness scale divided by the time scale). Since it is the rapid evaporation that mainly causes the interfacial displacement, we can write it as

$$\left(\frac{\mathrm{d}L}{\mathrm{d}t}\right)^* = \frac{1}{k_{\text{evap}}}\left(\frac{\mathrm{d}L}{\mathrm{d}t}\right) \tag{22}$$

The scale factors in Eqs. (20)–(22) result in the following set of dimensionless describing equations, along with the corresponding dimensionless groups.

$$\left(\frac{L_{SC}^2}{t_\circ D_{\text{PSC}}}\right)\frac{\partial\omega_{\text{PSC}}^*}{\partial t^*} = \frac{\partial}{\partial z_{SC}^*}\left[\frac{1}{(1-\omega_P^{SC})^*}\frac{\partial\omega_{\text{PSC}}^*}{\partial z_{SC}^*}\right] \tag{23}$$

$$\left(\frac{L_{VT}^2}{t_o D_{\text{PVT}}}\right)\frac{\partial\omega_{\text{PVT}}^*}{\partial t^*} = \frac{\partial}{\partial z_{VT}^*}\left[\frac{1}{(1-\omega_P^{VT})^*}\frac{\partial\omega_{\text{PVT}}^*}{\partial z_{VT}^*}\right] \tag{24}$$

The initial and BCs are written as

$$\text{At } t^* = 0,\quad \omega_{\text{PSC}}^* = \omega_{\text{PVT}}^* = 0 \tag{25,26}$$

$$\text{At } z_{SC}^* = 1,\quad \omega_{\text{PSC}}^*|_{1,t^*} = 1\quad \text{for } 0 \leqslant t^* \leqslant \frac{t_{\text{depl}}}{t_o} \tag{27}$$

and

$$\frac{1}{(1-\omega_P^{SC})^*}\frac{\partial\omega_{\text{PSC}}^*}{\partial z_{SC}^*} = \left(\frac{k_{\text{evap}}}{P_{SC}}\right)\left(\frac{\rho_P^0}{\rho^{SC}}\right)\omega_{\text{PSC}}^*\Big|_{L_{SC}/z_{SCs},t^*}$$
$$\text{for } t^* \geqslant \frac{t_{depl}}{t_o} \tag{28}$$

where $P_{SC} = D_{\text{PSC}}K_{SC/VH}^P/L_{SC}$ represents the permeability of the permeant in the SC.

$$\text{At } z_{SC}^* = z_{VT}^* = 0,\quad \omega_{\text{PSC}}^*|_{0,t^*} = \omega_{\text{PVT}}^*|_{0,t^*} \tag{29}$$

$$\frac{1}{(1-\omega_P^{VT})^*}\frac{\partial\omega_{\text{PVT}}^*}{\partial z_{VT}^*} = \left(\frac{P_{SC}}{P_{VT}}\right)\frac{1}{(1-\omega_P^{SC})^*}\frac{\partial\omega_{\text{PSC}}^*}{\partial z_{SC}^*} \tag{30}$$

where $P_{VT} = D_{\text{PVT}}K_{VT/SC}^P K_{SC/VH}^P/L_{VT}$ is similarly the permeability of the permeant in the VT phase.

$$\text{At } z_{VT}^* = 1,\quad \omega_{\text{PSC}}^*|_{1,t^*} = \omega_{\text{PVT}}^*|_{1,t^*} = 0 \tag{31,32}$$

Finally, the coupled ODE is written as

$$\left(\frac{\mathrm{d}L}{\mathrm{d}t}\right)^* = -1 + \left(\frac{P_{SC}}{k_{\text{evap}}}\right)\left[\frac{1}{(1-\omega_P^{SC})^*}\frac{\partial\omega_{\text{PSC}}^*}{\partial z_{SC}^*}\right]\Bigg|_{z_{SC}^*=1} \tag{33}$$

with the corresponding dimensionless IC:

$$\text{at } t^* = 0,\quad L^* = 1 \tag{34}$$

The coefficients of the unsteady-state (first) terms in Eqs. (23) and (24) are the reciprocals of the respective Fourier numbers,

$$Fo_{SC} = \frac{t_o D_{\mathrm{PSC}}}{L_{SC}^2} \quad \text{and} \quad Fo_{VT} = \frac{t_o D_{\mathrm{PVT}}}{L_{VT}^2} \tag{35,36}$$

Eqs. (23) and (24) indicate that if the Fourier numbers are inherently large (for example, in thin barrier layers), the system will reach a steady state quickly. Also, at long times, the system will reach steady state as would be expected. According to $o(1)$ scaling analysis, if the Fourier numbers are greater than approximately 100, the unsteady state term can be dropped from the analysis and a quasi-steady state analysis is sufficient to accurately describe the process (Krantz, 1970, 2007). In such cases, the system can be appropriately described through the use of ODEs; even if these ODEs are non-linear (due to the presence of the convection term), they will be much simpler to integrate.

It is clear that for a combined evaporation–absorption process, the system response (particularly, the individual fractions of the applied liquid that evaporate and absorb) will depend on the evaporative mass-transfer coefficient and the permeabilities of the SC and VT. Scaling analysis reveals the nature of this dependence. In fact, the system behavior is dictated not by the absolute values of the system parameters, but by their values relative to each other, arranged specifically in terms of dimensionless groups, as shown in Eqs. (23)–(34). For instance, the rate of displacement of the liquid–air interface should depend on all the different mechanisms that cause the VH layer to shrink, which in this case are both evaporation and absorption into the SC, as shown in Eq. (33). Other than a few exceptions, the VT is much more permeable than the SC such that changes P_{SC} does not significantly alter the ratio P_{SC}/P_{VT}. In such cases, for a constant P_{VT}, the ratio of evaporated and absorbed fractions of the applied amount of liquid (henceforth referred to as 'disposition ratio') should depend only on the ratio k_{evap}/P_{SC}. This ratio appears in Eqs. (28) and (33). If, however, P_{VT} varies, then even for a fixed value of k_{evap}/P_{SC}, the ratio P_{SC}/P_{VT} and, as a result the disposition ratio will vary. In accordance with the conventional nomenclature in the engineering literature, it may be called the disposition Biot number (Bi), representing a measure of the evaporation of the compound into the surrounding gaseous phase relative to its diffusion into the SC. Thus, we have

$$Bi = \frac{k_{\mathrm{evap}}}{P_{SC}} \tag{37}$$

It should be noted that a dimensionless group (χ), conceptually similar to this Biot number and representing the relative evaporation–absorption tendency, had been introduced in the KM model (Kasting and Miller, 2006).

In the current system, the SC and VT offer resistances to permeation in series and the equivalent permeability (P_{EQ}) of the system is given as

$$\frac{1}{P_{\mathrm{EQ}}} = \frac{1}{P_{SC}} + \frac{1}{P_{VT}} \tag{38}$$

Eq. (38) can be rewritten as

$$\frac{P_{SC}}{P_{EQ}} = 1 + \frac{1}{P_R} \tag{39}$$

where the relative permeability (P_R) is given as

$$P_R = \frac{P_{VT}}{P_{SC}} \tag{40}$$

The dimensionless group P_R is similar to the parameter B introduced by Cleek and Bunge (1993) representing the relative permeability of SC and epidermis. It is clear from Eq. (39) that for large values of P_R, P_{EQ} will be nearly equal to P_{SC}. The $o(1)$ scaling analysis predicts that for P_R values greater than approximately 100, the presence of the VT will be virtually undetectable. In this case, a monolayer skin model (with only a SC) is sufficient to describe the permeation characteristics for that particular permeant. On the other hand, if P_R is less than approximately 100, it should be included in the analysis. Also, Eq. (33) shows that the interfacial displacement velocity (slope of the curve depicting changing VH layer thickness with time) will depend on Bi. For Bi values greater than or equal to approximately 100, the second term in the right-hand side of Eq. (33) will be negligibly small. In this case, evaporation dominates the skin disposition process and the change of the VH thickness due to permeation of permeant into the SC is negligible compared to evaporation at the free surface. In such cases, the normalized slope is equal to -1 at all times. However, for Bi values less than approximately 100, this term cannot be neglected. In such cases, the magnitude of the slope is significantly larger than -1 and its magnitude increases progressively with decreasing Bi. In the case where k_{evap} is negligibly small, Eq. (33) is not valid and Eq. (19) must be rescaled to obtain a different expression since k_{evap} is no longer a good scale for the interfacial displacement velocity. However, for volatile solvents k_{evap} is sufficiently large that this situation does not occur.

4. Solution methodology

Eqs. (1)–(19) were solved numerically using a finite difference/finite element-based subroutine D03PPF from the NAG® (Numerical Algorithms Group) mathematical library (NAG®). The solution is obtained using the method of lines. The PDEs are discretized in space, and the resulting ODEs are integrated in time

Table 1
Model equations for transformed coordinate system

$$\frac{\partial \omega_P^{SC}}{\partial t} = \frac{D_{\mathrm{PSC}}}{L_{SC}^2} \frac{\partial}{\partial z^{SC}} \left[\frac{1}{(1-\omega_P^{SC})} \frac{\partial \omega_P^{SC}}{\partial z^{SC}} \right] \tag{43}$$

$$\frac{\partial \omega_P^{VT}}{\partial t} = \frac{D_{PVT}}{L_{VT}^2} \frac{\partial}{\partial z^{VT}} \left[\frac{1}{(1-\omega_P^{VT})} \frac{\partial \omega_P^{VT}}{\partial z^{VT}} \right] \tag{44}$$

$$\omega_P^{VT}|_{z^{VE},0} = 0c \tag{45}$$

$$\omega_P^{SC}|_{z^{SC},0} = 0 \quad \text{for } 0 \leqslant z^{SC} < 1 - f_{\mathrm{dep}} \tag{46}$$

$$\omega_P^{SC}|_{z^{SC},0} = \omega_{\mathrm{sat}}^0 \quad \text{for } 1 - f_{\mathrm{dep}} \leqslant z \leqslant 1 \tag{47}$$

$$\omega_P^{VE}|_{1,t} = 0 \tag{10}$$

$$\omega_P^{SC}|_{1,t} = K_{SC/VH}^p \frac{\rho_P^0}{\rho^{SC}} \quad \text{for } 0 \leqslant t \leqslant t_{\mathrm{depl}} \tag{11}$$

$$\left. \frac{\rho^{SC} D_{\mathrm{PSC}}}{L_{SC}(1-\omega_P^{SC})} \frac{\partial \omega_P^{SC}}{\partial z^{SC}} \right|_{1,t} = k_{\mathrm{evap}} \rho_P^0 (\omega_P^{SC}|_{1,t}) \quad \text{for } t \geqslant t_{\mathrm{depl}} \tag{48}$$

$$\left. \frac{\rho^{VT} D_{\mathrm{PVT}}}{L_{VT}(1-\omega_P^{VT})} \frac{\partial \omega_P^{VT}}{\partial z^{VT}} \right|_{0,t} = \left. \frac{\rho^{SC} D_{\mathrm{PSC}}}{L_{SC}(1-\omega_P^{SC})} \frac{\partial \omega_P^{SC}}{\partial z^{SC}} \right|_{0,t} \tag{49}$$

$$\rho_P^o \frac{\mathrm{d}L}{\mathrm{d}t} = -k_{\mathrm{evap}} \rho_P^o + \left. \frac{\rho^{SC} D_{\mathrm{PSC}}}{L_{SC}(1-\omega_P^{SC})} \frac{\partial \omega_P^{SC}}{\partial z^{SC}} \right|_{z^{SC}=1} \tag{50}$$

using the Gear method, which is suited for stiff problems for which the temporal gradients can be very large. Trial simulations were performed with increasing mesh sizes. A mesh size of 201 nodes was determined to have sufficient numerical accuracy and was used to generate the simulation results reported here.

Although D03PPF can solve multiple PDEs, an important restriction lies in the fact that the spatial location of the boundaries (on which BC are imposed) for all the individual PDEs in the system must be the same (They are represented in the NAG® manual (NAG®, 2006) as $x = a$ and $x = b$.) This condition must be satisfied irrespective of the system of equations, even if the equations involve several layers having different thicknesses. In the model developed here the transport equations involve three distinct layers, the VH, SC and VT, each having a different thickness. Hence, the model equations cannot be solved in their original form. Eqs. (5)–(19) must first be rewritten through a process of compression and normalization of all the skin layers. This can be achieved by converting the spatial coordinate (z) from a uniform variable to a layer-specific variable, using the following set of transformation equations:

$$z^{SC} = \frac{z}{L_{SC}} \tag{41}$$

$$z^{VT} = -\frac{z}{L_{VT}} \tag{42}$$

Eqs. (41) and (42) can be used to develop specific equations relating the expressions for partial derivatives between the old and the new coordinate systems. Using these expressions, the model equations can be rewritten for the transformed coordinate system. These equations are given in Table 1.

5. Representative results

A detailed validation of the proposed model requires real-time experimental data on skin permeation of pure volatile liquids. The data-acquisition technique that has been employed for studying the current percutaneous absorption process is described in an accompanying paper (Ray Chaudhuri et al., 2009). In this section, the model predictions and their implications are presented through representative simulations. The system behavior of the proposed model is similar to the KM model (Kasting and Miller, 2006) as well as related modeling efforts from other groups (Anissimov and Roberts, 1999, 2001; Fernandes et al., 2005). Hence, this section will present key simulation results in order to highlight the system behavior and will not revisit the model implications already established in the KM model (Kasting and Miller, 2006).

The skin permeation model developed here is capable of predicting the concentration profiles inside the SC and VT, the instantaneous VH thickness, the instantaneous evaporation and absorption fluxes, and the cumulative amounts (representing the fraction of the original dose) of the evaporation and absorption fluxes, as well as other quantities that are useful for interpreting the process. Each of these quantities has special significance depending on the particular field of study. The most relevant and important indicator for occupational safety and health is the total amount of liquid penetrated through the skin, as given by the fraction of the applied dose absorbed. For studies pertaining to pharmacokinetic bioequivalence, several other quantities such as the maximum absorption flux of the permeant (peak flux) and the time required to reach this peak flux are important (Anissimov and Roberts, 2001). Furthermore, for toxicological studies pertaining to allergic contact dermatitis (ACD), the epidermal concentrations are critically important (more than the absorption flux or amount penetrated). Also, for studies pertaining to efficacy and product development of volatile ingredients in fragranced products and insect repellants, the instantaneous evaporation flux is the relevant quantity. Properties of the system such as the instantaneous thickness of the VH and concentration profiles of the permeant inside the SC and VT are extremely difficult to measure experimentally and results pertaining to these quantities are rare in the literature. Thus, the validation of the model predictions for these quantities involves a considerable effort that may not be warranted for volatile organic solvents. Systems that do warrant such attention due to their commercial importance include water concentration profiles in the SC (for cosmetic benefits) (Warner et al., 1988; Bouwstra et al., 2003) and allergen concentration in the VT (Basketter et al., 2007). It is of interest to note that volatile permeants, including ethanol, are predicted to have concentration maxima within the skin once the VH has evaporated, due to simultaneous loss from the upper and lower surfaces. Such profiles are easily studied with the mass-transport model developed in this paper (model predictions not shown).

Table 2
Numerical values of physical and transport properties for the ethanol/SC/VT system

Parameter	Symbol	Value (units)
Pure ethanol density	ρ^{VH}	780.8 kg/m^3
Molecular weight of ethanol	MW	46.07 g/gmol
Pure SC density @ 30% w/w H_2O	ρ^{SC}	1193.6 kg/m^3
Thickness of the SC	L_{SC}	1.34×10^{-5} m
Diffusivity of ethanol in SC	D_{PSC}	4.6455×10^{-14} m^2/s
Pure VT density	ρ^{VT}	1019.0 kg/m^3
Thickness of the VT	L_{VT}	5.00×10^{-4} m
Diffusivity of ethanol in VT	D_{PVT}	5.7100×10^{-10} m^2/s
SC/VH partition coefficient of ethanol	$K^p_{SC/VH}$	0.3029
VT/SC partition coefficient of ethanol	$K^p_{VT/SC}$	2.3308
Evaporation mass-transfer coefficient for ethanol	k_{evap}	1.063×10^{-6} m/s
Constant system temperature		32 °C

As discussed earlier, the fraction absorbed depends only on the ratio of the evaporative mass-transfer coefficient and the overall permeability of the skin sub-layers. However, a change in the absolute value of the latter will change both the peak flux and time to reach that peak flux. For a given permeant, the experimental parameters that can be varied freely are the initial amount of the liquid (also referred to as the dose), the ambient airflow velocity (which affects the evaporative mass-transfer coefficient) and the system temperature. This article restricts the representative simulations to variations in the airflow velocity and other experimental conditions, and for a particular compound, ethanol. Ethanol was the diluent used in earlier studies of our research group of the less volatile compounds DEET (Santhanam et al., 2005) and benzyl alcohol (Miller et al., 2006). In order to interpret the binary system behavior in these studies, the kinetics of both solute and the solvent must be understood. The accompanying paper (Ray Chaudhuri et al., 2009) provides details on how to estimate the thermodynamic and transport properties for the ethanol–skin system. The numerical values used here (Table 2) were chosen to approximately represent the situation of ethanol permeation through human skin. The influence of the fractional deposition depth (f_{dep}) will be examined in some detail since this parameter is a relatively new concept that has not been extensively evaluated. The usefulness of f_{dep} is reinforced in the accompanying experimental study of ethanol–skin permeation (Ray Chaudhuri et al., 2009).

5.1. Dose dependence

The scaling analysis predicts that when $f_{dep} = 0$, the fraction absorbed at steady state should depend only on Bi and not on dose. It may also seem from Eqs. (23)–(34) that the dimensionless Fourier numbers would have an effect on the fraction absorbed. Fourier numbers are associated with the time derivatives in the describing PDEs are indicative of transient phenomena. However, the total amount (or fraction) absorbed is not a transient property of the system but a cumulative quantity integrated over time that should not depend on the Fourier numbers. To test this dose dependence, we conducted

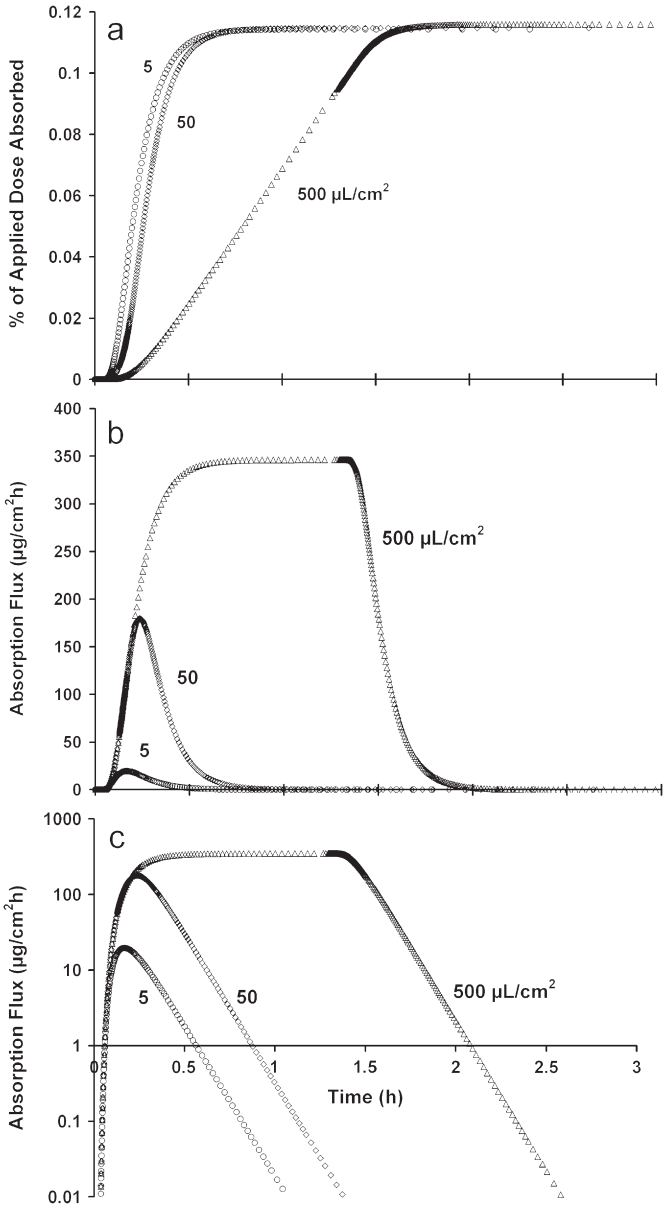

Fig. 2. Cumulative and instantaneous absorption flux profiles with varying doses (5, 50 and 500 μL/cm^2): (a) cumulative absorption; (b) instantaneous absorption flux; (c) absorption flux plotted on a logarithmic scale. The value $f_{dep} = 0$ was employed for these calculations.

simulations using the parameters in Table 2 and doses of 5, 50 and 500 μL/cm^2, which correspond to initial VH thicknesses of 50, 500 and 5000 μm. Fig. 2 shows the results. Although the shapes of the flux profiles (Fig. 2b) including the peak flux and time to reach the peak flux are different, the fractions of dose absorbed at steady state are the same for all doses (Fig. 2a). The system reaches a steady state for the 500 μL/cm^2 dose, but not for the smaller doses. Similar results have been obtained in prior modeling studies (Anissimov and Roberts, 1999, 2001; Kasting and Miller, 2006). Also, at long times the absorption flux should decay exponentially (Anissimov and Roberts, 1999, 2001). This behavior can be clearly seen in Fig. 2c, which shows a plot of the logarithm of the absorption flux as a function of time. As noted by Anissimov and Roberts (2001), the slope of the linear portion of the curves in Fig. 2c is a function only of the intrinsic permeabilities of the SC and VT. For a given permeant, the slope remains constant, even if the dose is varied. Fig. 2c confirms this prediction.

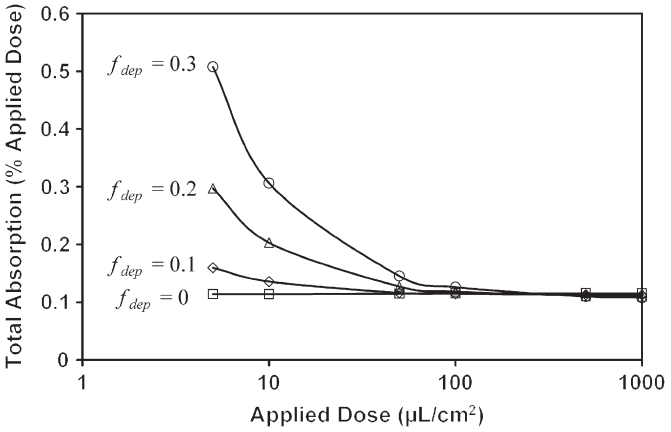

Fig. 3. Variation of total absorbed fraction with applied dose for varying values of deposition depth (f_{dep}).

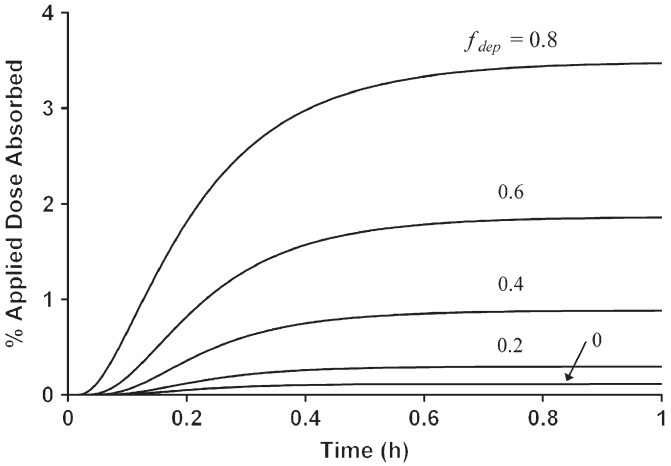

Fig. 4. Profiles for cumulative absorption with varying f_{dep}. A dose of 5 μL/cm^2 was assumed in the calculations.

When f_{dep} is non-zero, the cumulative absorption depends on dose as shown in Fig. 3, which shows a plot of the total absorption as a function of applied dose. This result stems from the fact that small doses deposited into the upper SC evaporate more slowly than solvent residing in the VH layer. For very large doses (greater than approximately 100 μL/cm^2), the system is insensitive to the numerical value of f_{dep}. This reflects the fact that the VH layer persists for an extended time under these conditions, so that the initial deposition of a small fraction of the solvent into the upper SC is inconsequential. Values of f_{dep} for ethanol in the range 0.1–0.3 were derived from experimental skin absorption data by regression analysis (Ray Chaudhuri et al., 2009). It should be noted that the strong dependence of absorption on f_{dep} shown in Fig. 3 is a consequence of the high volatility of ethanol. Less volatile permeants show much weaker relationships (Santhanam et al., 2005; Kasting and Miller, 2006; Miller et al., 2006; Kasting et al., 2008).

5.2. Deposition depth dependence

Fig. 4 shows the result of varying f_{dep} for a small applied dose (5 μL/cm^2). It is clear from the figure that for a smaller dose, the fraction absorbed is dose-dependent. For $f_{dep} = 1$, the maximum absorbed fraction was calculated to be 5.5%. Thus, contrary to the situation where $f_{dep} = 0$, the total absorbed fraction is not constant

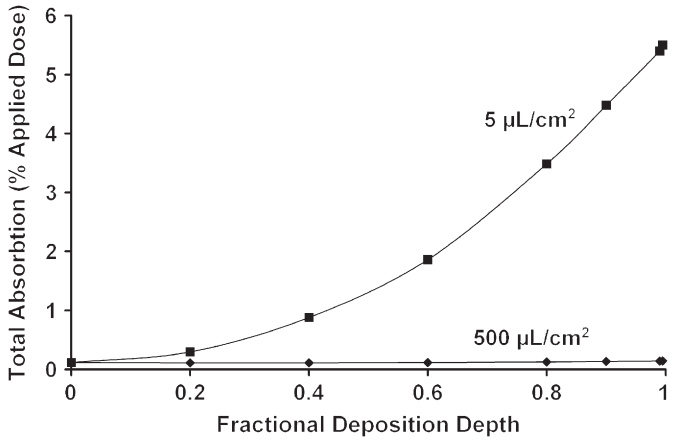

Fig. 5. Total absorbed fraction as a function of f_{dep} for small (5 μL/cm²) and large (500 μL/cm²) doses.

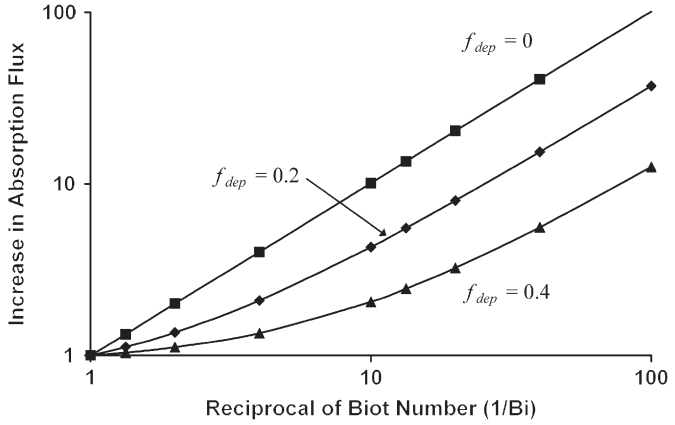

Fig. 6. Variation in absorption flux with *Bi* for different values of f_{dep}. The dose assumed in the calculation was 50 μL/cm².

although the value of *Bi* remains the same. Fig. 5 shows the simulation results using a substantially larger dose (500 μL/cm²). Similar to the finding in Fig. 3, f_{dep} does not have a major impact on the total absorbed fraction for the larger dose.

5.3. Airflow dependence

For a particular permeant and a constant temperature, the evaporation mass-transfer coefficient (k_{evap}) is a function only of the airflow velocity. The default value of k_{evap} representing laboratory conditions in a fume hood is 0.38 cm/h (as given in Table 1), corresponding to an airflow velocity of 0.74 m/s. In these simulations, k_{evap} was varied to be 0.1, 1 and 10 times the default value. This changes only the *Bi* without altering the Fourier numbers of either skin layers. The applied dose for these simulations was 50 μL/cm². Initially the value $f_{dep} = 0$ was chosen, which meant that an increase in k_{evap} should yield a proportional decrease in the total absorbed fraction. In other words, if the total absorbed fraction is plotted against the reciprocal of *Bi* (both quantities on a logarithmic scale) the result should be a straight line with slope = 1. This result is evident from the solid squares in Fig. 6. However, this proportional change is observed only when f_{dep} is zero. For non-zero f_{dep}, the relative absorption flux increase is less for a given value of 1/*Bi*. This effect is more prominent for higher deposition depths.

6. Conclusions

A mathematical model representing transient mass-transfer pertaining to skin permeation of pure volatile liquids was presented in this paper. For small doses the model is sensitive to a parameter defined as the fractional deposition depth of permeant in the SC (f_{dep}), which mathematically appears in the ICs for the problem. The system behavior is found to be in accordance with the predictions of scaling analysis as well as with several analytical results in the literature. The simulation results indicated that the total amount of a topically applied compound permeating through the skin depends on the temperature, the vapor pressure of the permeant, the ambient airflow velocity, the permeability of the SC and VT, and on the fractional deposition depth (f_{dep}). For a given permeant, the fraction of dose absorbed depends only on system temperature, airflow velocity, dose and f_{dep}. The proposed model can be used to predict percutaneous disposition characteristics for pure volatile liquids and can also be extended to non-volatile liquids.

Acknowledgments

The authors acknowledge financial support through the National Institute for Occupational Safety & Health (Grant R01 OH007529). They also greatly appreciate the help on NAG® subroutines by Dr. Hanyong Lee of the Samsung Engineering Company Ltd., Republic of Korea.

References

Alsoy, S., Duda, J.L., 2002. Influence of swelling and diffusion-induced convection on polymer sorption processes. A.I.Ch.E. Journal 48, 1849–1855.

Anissimov, Y.G., Roberts, M.S., 1999. Diffusion modeling of percutaneous absorption kinetics: 1. Effects of flow rate, receptor sampling rate, and viable epidermal resistance for a constant donor concentration. Journal of Pharmaceutical Sciences 88, 1201–1209.

Anissimov, Y.G., Roberts, M.S., 2001. Diffusion modeling of percutaneous absorption kinetics: 2. Finite vehicle volume and solvent deposited solids. Journal of Pharmaceutical Sciences 90, 504–520.

Anissimov, Y.G., Roberts, M.S., 2004. Diffusion modeling of percutaneous absorption kinetics: 3. Variable diffusion and partition coefficients, consequences for stratum corneum depth profiles and desorption kinetics. Journal of Pharmaceutical Sciences 93, 470–487.

Barbero, A.M., Frasch, H.F., 2005. Modeling of diffusion with partitioning in stratum corneum using a finite element model. Annals of Biomedical Engineering 33, 1281–1292.

Basketter, D.A., Pease, C., Kasting, G.B., Kimber, I., Casati, S., Cronin, M.T.D., Diembeck, W., Gerberick, G.F., Hadgraft, J., Hartung, T., Marty, J.P., Nikolaidis, E., Patlewicz, G.Y., Roberts, D., Roggen, E., Rovida, C., van de Sandt, H., 2007. Skin sensitisation and epidermal disposition. The relevance of epidermal bioavailability for sensitisation hazard identification/risk assessment. Alternatives to Laboratory Animals 35, 137–154.

Batterman, S.A., Franzblau, A., 1997. Time-resolved cutaneous absorption and permeation rates of methanol in human volunteers. International Archives of Occupational and Environmental Health 70, 341–351.

Bear, J., Bachmat, Y., 1990. Introduction to Modeling of Transport Phenomena in Porous Media. Kluwer Academic Publishers, Boston.

Bird, R.B., Stewart, W.E., Lightfoot, E.N., 1960. Transport Phenomena. Wiley, New York.

Blank, I.H., 1964. Penetration of low-molecular-weight alcohols into skin. I. Effect of concentration of alcohol and type of vehicle. Journal of Investigative Dermatology 43, 415–420.

Bouwstra, J.A., Honeywell-Nguyen, P.L., Gooris, G.S., Ponec, M., 2002. Structure of the skin barrier and its modulation by vesicular formulations. Progress in Lipid Research 42, 1–36.

Bouwstra, J.A., de Graaff, A., Gooris, G.S., Nijsse, J., Wiechers, J.W., van Aelst, A.C., 2003. Water distribution and related morphology in human stratum corneum at different hydration levels. Journal of Investigative Dermatology 120, 750–758.

Cleek, R.L., Bunge, A.L., 1993. A new method for estimating dermal absorption from chemical exposure. 1. General approach. Pharmaceutical Research 10, 497–506.

Cussler, E.L., 1997. Diffusion: Mass Transfer in Fluid Systems. Cambridge University Press, Cambridge. Chapter 3, pp. 50–78.

Deen, W.M., 1998. Analysis of Transport Phenomena. Oxford University Press, New York.

Del-Valle, V., Almenar, E., Hernández-Muñoz, P., Lagarón, J.M., Catala, R., Gavara, R., 2004. Volatile organic compound permeation through porous polymeric films

for modified atmosphere packaging of foods. Journal of the Science of Food and Agriculture 84, 937–942.
Fernandes, M., Simon, L., Loney, N.W., 2005. Mathematical modeling of transdermal drug-delivery systems: analysis and applications. Journal of Membrane Science 256, 184–192.
Fiedler, M., Meier, W.-D., Hoppe, U., 1995. Texture analysis of the surface of the human skin. Skin Pharmacology 8, 252–265.
Fischer, T.W., Wigger-Alberti, W., Elsner, P., 1999. Direct and non-direct measurement techniques for analysis of skin surface topography. Skin Pharmacology and Applied Physiology 12, 1–11.
Flynn, G.L., 1990. Physicochemical determinants of skin absorption. In: Gerritv, T.R., Henry, C.J. (Eds.), Principles of Route-to-Route Extrapolation for Risk Assessment. Elsevier, New York, pp. 93–127.
Frasch, H.F., 2002. A random walk model of skin permeation. Risk Analysis 22, 265–276.
Frasch, H.F., Barbero, A.M., 2003. Steady-state flux and lag time in the stratum corneum lipid pathway: results from finite element models. Journal of Pharmaceutical Sciences 92, 2196–2207.
Fujimura, T., Haketa, K., Hotta, M., Kitahara, T., 2007. Global and systematic demonstration for the practical usage of a direct in vivo measurement system to evaluate wrinkles. International Journal of Cosmetic Science 29, 423–436.
Geinoz, S., Guy, R.H., Testa, B., Carrupt, P.-A., 2004. Quantitative structure–permeability relationships (QSPeRs) to predict skin permeation: a critical evaluation. Pharmaceutical Research 21 (1), 83–92.
Jakasa, I., Mohammadi, N., Krüse, J., Kezic, S., 2004. Percutaneous absorption of neat and aqueous solutions of 2-butoxyethanol in volunteers. International Archives of Occupational and Environmental Health 77, 79–84.
Kasting, G.B., 2001. Kinetics of finite dose absorption through skin: 1. Vanillylnonanamide. Journal of Pharmaceutical Sciences 90, 202–212.
Kasting, G.B., Miller, M.A., 2006. Kinetics of finite dose absorption through skin: 2. Volatile compounds. Journal of Pharmaceutical Sciences 95, 268–280.
Kasting, G.B., Miller, M.A., Bhatt, V., 2008. A spreadsheet-based method for estimating the skin disposition of volatile compounds: application to *N*,*N*-diethyl-m-toluamide (DEET). Journal of Occupational and Environmental Hygiene 10, 633–644.
Kezic, S., Monster, A.C., Krüse, J., Verberk, M.M., 2000. Skin absorption of some vaporous solvents in volunteers. International Archives of Occupational and Environmental Health 73, 415–422.
Korinth, G., Geh, S., Schaller, K.H., Drexler, H., 2003. In vitro evaluation of the efficacy of skin barrier creams and protective gloves on percutaneous absorption of industrial solvents. International Archives of Occupational and Environmental Health 76, 382–386.
Krantz, W.B., 1970. Scaling initial and boundary value problems as a teaching tool for a course in transport phenomena. Chemical Engineering Education 4, 145.
Krantz, W.B., 2007. Scaling Analysis in Modeling Transport and Reaction Processes: A Systematic Approach to Model Building and the Art of Approximation. Wiley, Hoboken, NJ.
Krantz, W.B., Sczechowski, J.G., 1994. Scaling initial and boundary value problems: a tool in engineering teaching and practice. Chemical Engineering Education 28, 236–253.
Larese Filon, F., Fiorito, A., Adami, G., Barbieri, P., Coceani, N., Bussani, R., Reisenhofer, E., 1999. Skin absorption in vitro of glycol ethers. International Archives of Occupational and Environmental Health 72, 480–484.
Lee, H., Ray Chaudhuri, S., Krantz, W.B., Hwang, S.-T., 2006. A model for evaporative casting of polymeric membranes incorporating convection due to density changes. Journal of Membrane Science 284, 161–172.
Lockley, D.J., Howes, D., Williams, F.M., 2004. Percutaneous penetration and metabolism of 2-butoxyethanol. Archives of Toxicology 78, 617–628.
McCarley, K.D., Bunge, A.L., 2001. Pharmacokinetic models of dermal absorption. Journal of Pharmaceutical Sciences 90, 1699–1719.
Menon, G., 2002. New insights into skin structure: scratching the surface. Advanced Drug Delivery Reviews 54 (Suppl. 1), S3–S17.
Miller, M.A., Bhatt, V., Kasting, G.B., 2006. Dose and airflow dependence of benzyl alcohol disposition on skin. Journal of Pharmaceutical Sciences 95, 281–291.
Montagna, W., Kligman, A.M., Carlisle, K.S., 1992. Atlas of Normal Human Skin. Springer, Berlin, Heidelberg.
Moss, G.P., Dearden, J.C., Patel, H., Cronin, M.T.D., 2002. Quantitative structure—permeability relationships (QSPRs) for percutaneous absorption. Toxicology in Vitro 16, 299–317.
Mráz, J., Nohová, H., 1992. Percutaneous absorption of *N*,*N*-dimethylformamide in humans. International Archives of Occupational and Environmental Health 64, 79–83.
Potts, R.O., Francoeur, M.L., 1991. The influence of stratum corneum morphology on water permeability. Journal of Investigative Dermatology 96, 495–499.
Potts, R.O., Guy, R.H., 1992. Predicting skin permeability. Pharmaceutical Research 9, 663–669.
Ray Chaudhuri, S., Gajjar, R.M., Krantz, W.B., Kasting, G.B., 2009. Percutaneous absorption of volatile solvents following transient liquid exposures. II. Ethanol. Chemical Engineering Science, submitted for publication.
Roberts, M.S., Walters, K.A., 1998. In: Roberts, M.S., Walters, K.A. (Eds.), The Relationship between Structure and Barrier Function of Skin. Marcel Dekker Inc., New York.
Santhanam, A., Miller, M.A., Kasting, G.B., 2005. Absorption and evaporation of *N*,*N*-diethyl-*m*-toluamide from human skin in vitro. Toxicology and Applied Pharmacology 204, 81–90.
Scheuplein, R.J., 1965. Mechanism of percutaneous drug absorption. I: routes of penetration and the influence of solubility. Journal of Investigative Dermatology 45, 334–345.
Scheuplein, R.J., Blank, I.H., 1971. Permeability of the skin. Physiological Reviews 51, 702–747.
Semple, S., Brouwer, D.H., Dick, F., Cherrie, J.W., 2001. A dermal model for spray painters. Part II: estimating the deposition and uptake of solvents. Annals of Occupational Hygiene 45, 25–33.
Singh, S., Singh, J., 1993. Transdermal drug delivery by passive diffusion and iontophoresis: a review. Medicinal Research Reviews 13, 569–621.
Stinchcomb, A.L., Pirot, F., Touraille, G.D., Bunge, A.L., Guy, R.H., 1999. Chemical uptake into human stratum corneum in vivo from volatile and non-volatile solvents. Pharmaceutical Research 16, 1288–1293.
Warner, R.R., Myers, M.C., Taylor, D.A., 1988. Electron probe analysis of human skin: determination of water concentration profile. Journal of Investigative Dermatology 90, 218–224.
Wilkinson, S.C., Williams, F.M., 2002. Effects of experimental conditions on absorption of glycol ethers through human skin in vitro. International Archives of Occupational and Environmental Health 75, 519–527.
Yamashita, F., Hashida, M., 2003. Mechanistic and empirical modeling of skin permeation of drugs. Advanced Drug Delivery Reviews 55, 1185–1199.